Available online at www.sciencedirect.com
SCIENCE DIRECT®
Journal of Theoretical Biology 233 (2005) 363–377
Journal of Theoretical Biology
www.elsevier.com/locate/yjtbi

The geometric theory of adaptive evolution: trade-off and invasion plots

Roger G. Bowers[a,*], Andrew Hoyle[a], Andrew White[b], Michael Boots[c]

[a]Department of Mathematical Sciences, Division of Applied Mathematics, Mathematical Sciences Building, The University of Liverpool, Liverpool, L69 3BX, UK
[b]Mathematics, School of Mathematical and Computer Sciences, Heriot Watt University, Edinburgh, EH14 4AS, UK
[c]Department of Animal and Plant Sciences, The University of Sheffield, Western Bank, Sheffield, S10 2TN, UK

Received 15 June 2004; received in revised form 11 October 2004; accepted 13 October 2004
Available online 8 December 2004

Abstract

The purpose of this paper is to take an entirely geometrical path to determine the evolutionary properties of ecological systems subject to trade-offs. In particular we classify evolutionary singularities in a geometrical fashion. To achieve this, we study trade-off and invasion plots (TIPs) which show graphically the outcome of evolution from the relationship between three curves. The first invasion boundary (curve) has one strain as resident and the other strain as putative invader and the second has the roles of the strains reversed. The parameter values for one strain are used as the origin with those of the second strain varying. The third curve represents the trade-off. All three curves pass through the origin or tip of the TIP. We show that at this point the invasion boundaries are tangential. At a singular TIP, in which the origin is an evolutionary singularity, the invasion boundaries and trade-off curve are all tangential. The curvature of the trade-off curve determines the region in which it enters the singular TIP. Each of these regions has particular evolutionary properties (EUS, CS, SPR and MI). Thus we determine by direct geometric argument conditions for each of these properties in terms of the relative curvatures of the trade-off curve and invasion boundaries. We show that these conditions are equivalent to the standard partial derivative conditions of adaptive dynamics. The significance of our results is that we can determine whether the singular strategy is an attractor, branching point, repellor, etc. simply by observing in which region the trade-off curve enters the singular TIP. In particular we find that, if and only if the TIP has a region of mutual invadability, is it possible for the singular strategy to be a branching point. We illustrate the theory with an example and point the way forward.

Keywords: Adaptive evolution; Trade-off; Invadability criterion; Evolutionary singularity; Predator–prey

1. Introduction

In this article, we develop a geometric theory of adaptive evolution subject to trade-offs. The theory is not explicitly genetic; it is constructed at the level of strains which are distinguished by the values of relatively few parameters. It is these parameters that are connected by trade-offs. Evolution is taken to proceed by local mutation and selection based on fitness calculated as the per capita growth rate of a mutant strategy in an environment determined by the resident population. We develop the theory in an ab initio, directly geometric manner using trade-off and invasion plots (TIPs) which are introduced below; in particular our approach differs markedly from the standard approach of 'adaptive dynamics' characterized by pairwise invadability plots or PIPs (Dieckmann and Law, 1996; Geritz et al., 1997, 1998; Metz et al., 1996). Our intention is to keep trade-offs firmly at the forefront and to argue directly from the geometry of TIPs to the

*Corresponding author. Tel.: +44 151 794 3780; fax: +44 151 794 4061.
E-mail address: sx04@liv.ac.uk (R.G. Bowers).

0022-5193/$ - see front matter © 2004 Elsevier Ltd. All rights reserved.
doi:10.1016/j.jtbi.2004.10.017

evolutionary properties. This reveals the origin and significance of the geometrical criteria in an immediate fashion. An alternative is to accept the known results of adaptive dynamics (Geritz et al., 1997, 1998; Metz et al., 1996) and apply them in the present context; with this procedure the geometrical consequences for TIPs emerge rather indirectly. We discuss the equivalence of the two approaches later in this article. Of course, in making an analysis based on TIPs, we acknowledge that we adopt the modelling framework, assumptions and concepts established in the pioneering articles on adaptive dynamics referenced above.

We particularize to a description involving trade-offs due to their importance in evolutionary theory (Boots and Begon, 1993; Stearns, 1992); energetic or other constraints require that a gain in one area of a species' life history must be bought at the cost of a loss in another. We represent trade-offs mathematically by linking pairs of parameters appearing in the theory by an explicit functional relationship. Another less explicit way of introducing them is often employed (see, for example, Doebeli et al., 2000; Kisdi, 1999; Marrow et al., 1996); here parameters are linked through a relationship with trait values. Previous theoretical studies using the more explicit functional route have applied the standard approach of adaptive dynamics in particular contexts. Bowers and White (2002) considered Lotka–Volterra systems in which all the parameters—except those linked by the trade-off—are independent. White and Bowers (2004) extended this to allow for inter-specific parameter dependence. Studies using more complex specific models that include parameter trade-offs have investigated the evolution of resistance to parasites (Boots and Haraguchi, 1999), the evolution of polymorphism in Levene-type models (Kisdi, 2001) and the role of explicit versus emergent carrying capacities in predator–prey models (Bowers et al., 2003). Gatto (1993) considered an evolutionary problem in which the feasibility set for the parameters played a central role. The intention here is to work within a framework using trade-offs but with the primary purpose of establishing a new theoretical perspective—which we shall naturally illustrate with examples.

Geometric plots representing invasion boundaries between pairs of interacting strains have been used to discuss the evolution of host resistance to microparasites (Antonovics and Thrall, 1994; Boots and Bowers, 1999, 2004; Bowers et al., 1994). In the latest of these articles, we introduced the idea of adding trade-off curves to our plots and hence arrived at the notion of TIPS. We also outlined very briefly a few of the results presented here. Two other groups have addressed similar problems from different points of view (Rueffler et al., 2004; De Mazancourt and Dieckmann, 2004).

The three curves in a TIP are plotted in the space of the parameters connected by the trade-off and we use the parameter values for one strain as an origin with those of a second strain varying along the invasion boundaries (Fig. 1). On a TIP one of the invasion boundaries represents the demarcation between those areas in parameter space where the tip strain as resident can be invaded by the other strain as rare mutant; the other boundary is similar but involves the tip strain as rare mutant and the other strain as resident. In order to cover all possible strain pairs we imagine the origin as sliding along the trade-off curve with different TIPs being constructed in each case (Fig. 2). Because of the restriction to trade-offs—which are represented by monotonic curves—we need only consider two quadrants on each TIP; because otherwise each feasible strain pair would be represented twice we further reduce this to one quadrant with the origin at an upper corner or tip of the TIP. We construct a local theory—which it transpires is based on gradients and curvatures at the

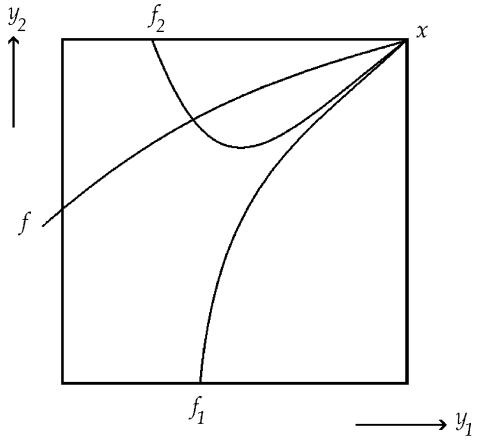

Fig. 1. An example of a TIP. Three curves are plotted in the space of the parameters connected by the trade-off and the parameter values for strain x are used as origin with those of a strain y varying on the axes. The curve f represents the trade-off between parameters. The curve f_1 represents the invasion boundary for strain x as resident and strain y as rare mutant; the other curve, f_2, is the invasion boundary for strain y as resident and strain x as rare mutant.

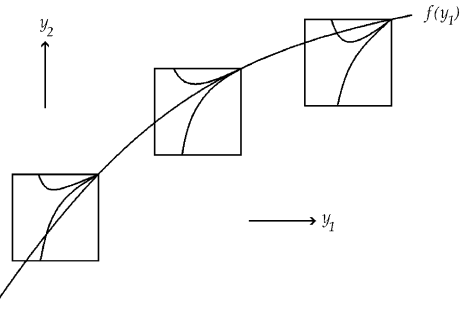

Fig. 2. A series of TIPs rooted at different points along the trade-off curve f. This construction allows all possible strain pairs to be considered.

origin, hence, inferences about the upper quadrant can be obtained without representing it explicitly.

The plan of the rest of this article is as follows. In the next section, we discuss the basic properties of TIPs and show that all the three curves pass through the tip and that the two invasion curves have a common gradient there. It follows that the outcomes of the interaction between two relatively similar strains are generically determined by the difference between this common gradient and the gradient of the trade-off curve at the tip of the appropriate TIP. Furthermore, we establish that evolutionary singularities are identified by the equality of all three gradients. In the following sections we focus on the singular TIP identified in this way and use it to characterize the usual properties—evolutionary unbeatability, spreading, convergence stability and mutual invadability (MI)—in a direct geometric fashion involving the relative curvatures of the three curves at the tip of the singular TIP. It follows that the nature of the evolutionary singularity (attractor, repellor, branching point, Garden of Eden point) is determined by these curvatures. In establishing these conclusions we do not use any of the standard derivative conditions of adaptive dynamics (although as acknowledged above we adopt the same basic assumptions). Thus in the next section we show how our curvature conditions relate to these derivative conditions, establishing in fact that (in the presence of trade-offs) the two approaches are equivalent. We then present an illustrative example of our approach using TIPs—we analyse prey evolution in a predator–prey model with a Holling type II functional response. This allows us to display different types of singular TIP and to check that corresponding simulations accord with our theory. We finish with a discussion section. We include an examination of the relationship between the present method of classifying singularities and the eight-fold way based on PIPs. We argue that the geometric method based on TIPs is of great utility both in presenting evolutionary theory and in discussing applications. An appendix collecting together some mathematical results is included.

2. Basic properties of trade-off and invasion plots (TIPS)

This study employs two fitness functions: $s_x(y)$ which dictates whether a rare (mutant) strategy y can invade a (resident) population x and $s_y(x)$ which dictates whether a rare (mutant) strategy x can invade a (resident) population y. When these two fitness functions have different signs, the outcome appears obvious. If $s_x(y)>0$ and $s_y(x)<0$, then y can invade x, but x cannot invade y, hence the x strategy will always be eliminated and the y strategy will 'win'. The opposite occurs when $s_x(y)<0$ and $s_y(x)>0$; then the x strategy will 'win'. (For a discussion of detailed conditions and results relating to these ideas see Dercole, 2002; Geritz, 2004; Geritz et al., 2002.)

For the TIP, we have two strategies x and y that can be defined by a large number of characterizing parameters with corresponding values x_i and y_i. However, as with previous studies (Bowers and White, 2002; Bowers et al., 2003; White and Bowers, 2004), as the strategies evolve, we take a majority of these parameters to remain constant, and only allow two to vary/evolve. Hence, the two strategies can be defined by these two evolving characteristics as $x=(x_1,x_2)$ and $y=(y_1,y_2)$. This implies that the two fitness functions above can be written in the form

$$s_x(y)=F(y_2,y_1,x_2,x_1), \tag{1}$$

$$s_y(x)=F(x_2,x_1,y_2,y_1). \tag{2}$$

The underlying fitness functions F, are identical. The first two parameters relate to the invading mutant strategy and the second two to the resident strategy. We use the fact that $s_x(x)=F(x_2,x_1,x_2,x_1)$ is zero to obtain

$$\begin{aligned} &F_1(x_2,x_1,x_2,x_1)+F_3(x_2,x_1,x_2,x_1)=0,\\ &F_2(x_2,x_1,x_2,x_1)+F_4(x_2,x_1,x_2,x_1)=0 \end{aligned} \tag{3}$$

and

$$\begin{aligned} &F_{11}(x_2,x_1,x_2,x_1)+2F_{13}(x_2,x_1,x_2,x_1)\\ &\quad+F_{33}(x_2,x_1,x_2,x_1)=0,\\ &F_{12}(x_2,x_1,x_2,x_1)+F_{14}(x_2,x_1,x_2,x_1)\\ &\quad+F_{23}(x_2,x_1,x_2,x_1)+F_{34}(x_2,x_1,x_2,x_1)=0,\\ &F_{22}(x_2,x_1,x_2,x_1)+2F_{24}(x_2,x_1,x_2,x_1)\\ &\quad+F_{44}(x_2,x_1,x_2,x_1)=0. \end{aligned} \tag{4}$$

(Two notational issues deserve attention. First, use of the symbol F for the underlying fitness function in (1) and (2) is presentationally convenient here—especially in equations (A.9)–(A.12). Second, we have used F_i to denote the derivative of F with respect to its ith argument.)

The two parameters defining each strategy are not taken to be independent; an improvement in the first characteristic must occur at a cost to the second. This trade-off between the parameters takes the form

$$y_2=f(y_1) \quad \text{and} \quad x_2=f(x_1). \tag{5}$$

We observe that f' will be of a fixed sign over the range of x_1 and y_1 by assumption, as a change in one parameter, whether increase or decrease, must also produce a change in the second parameter in a fixed direction. The introduction of this trade-off has the effect of allowing us now to define the strategies x and y, by a single evolving parameter x_1 and y_1. Substituting (5) into the fitness functions in (1) and (2), we get for x, y

restricted to the trade-off curve

$$s_x(y) = F(f(y_1), y_1, f(x_1), x_1), \tag{6}$$

$$s_y(x) = F(f(x_1), x_1, f(y_1), y_1). \tag{7}$$

Each of the two invasion boundaries on the TIP represent the values for y_1 and y_2 where the corresponding strategy has zero fitness. These boundaries divide the TIP into regions where the strategies x and y can and cannot invade the other strategy (respectively y and x). Formally, the boundaries are given from (1) and (2) and the second equation in (5) as follows:

$$s_x(y) = 0 \;\Leftrightarrow\; y_2 = \phi_1(y_1, x_2, x_1) = f_1(x_1, y_1), \tag{8}$$

$$s_y(x) = 0 \;\Leftrightarrow\; y_2 = \phi_2(y_1, x_2, x_1) = f_2(x_1, y_1), \tag{9}$$

where local uniqueness is guaranteed by assuming that the derivative of F with respect to its first argument does not vanish. Here, f_1 and f_2 are derived from ϕ_1 and ϕ_2 by restricting (x_1, x_2) to be on the trade-off curve $x_2 = f(x_1)$; no such restriction is imposed at this stage on (y_1, y_2). By substituting the relationships involving f_1 and f_2, from (8) and (9), in the fitness functions in (1) and (2), and also using $x_2 = f(x_1)$, we get the equalities

$$F(f_1(x_1, y_1), y_1, f(x_1), x_1) = 0, \tag{10}$$

$$F(f(x_1), x_1, f_2(x_1, y_1), y_1) = 0. \tag{11}$$

These equations are consistent with the observation that the two invasion boundaries and the trade-off must all pass through the tip of the TIP, $y_1 = x_1$, i.e.

$$f(x_1) = f_1(x_1, x_1) = f_2(x_1, x_1). \tag{12}$$

Furthermore, by calculating the derivatives of (10) and (11) with respect to y_1 (see (A.3) and (A.4) in the Appendix A) and evaluating them at the tip, we see that the two invasion boundaries will not only pass through this point, but also will have equal gradients there, (13). (We should note here that the various derivatives required throughout this paper are collected in the Appendix A.)

Although the trade-off curve passes through the tip, its gradient at this point will not in general be equal to those of the invasion boundaries. Hence, the trade-off will reach the tip by way of a path, either above or below the two invasion boundaries, depending on the strategy x. While the trade-off curve is on one side of the invasion boundaries locally near the tip, the first of the two strategies, x say, will win. As the TIP moves along the trade-off curve corresponding to varying the strategy x, there comes a point where the trade-off curve will pass from one side of the (mutually tangential) invasion boundaries to the other (see Fig. 2). After this point, the second strategy, y say, now wins. This point—or value of x—at which the trade-off is tangential to the invasion boundaries, is an *evolutionary singularity*, x^* (i.e. $x^* = (x_1^*, f(x_1^*))$, since there is a discontinuous change in the evolutionary properties. The corresponding TIP, for which $x = x^*$ is the tip, is called the *singular* TIP. In algebraic terms, on the singular TIP, we have

$$f'(x_1^*) = \left.\frac{\partial f_1}{\partial y_1}\right|_* = \left.\frac{\partial f_2}{\partial y_1}\right|_*, \tag{13}$$

where for notational convenience we use

$$|_* \Leftrightarrow |_{y=x=x^*}. \tag{14}$$

At the tip, the invasion boundaries quite generally have equal derivatives with respect to y_1. But what of the derivatives with respect to x_1? This dictates how the invasion boundaries change as the tip of the TIP is moved along the trade-off curve. By calculating the derivatives of (10) and (11) with respect to x_1 (giving (A.1) and (A.2) of the Appendix A), at the tip, assuming $F_1|_{y=x} \neq 0$, we find that the two invasion boundaries have equal rates of change with respect to x_1. However, adding to (A.1) the derivative of (10) with respect to y_1 (that is (A.3)) evaluated at the singularity and using (13), we find that the following result holds at the tip of the singular TIP (again assuming $F_1|_{y=x} \neq 0$):

$$\left.\frac{\partial f_1}{\partial x_1}\right|_* = 0 \quad \text{and} \quad \left.\frac{\partial f_2}{\partial x_1}\right|_* = 0. \tag{15}$$

This implies that for x close to x^*, the invasion boundaries remain unchanged up to first order. These results are important in allowing us to simplify many of the derivatives in the Appendix A.

3. The singular TIP

In order to discuss the nature of the evolutionary singularity we need to investigate the singular TIP. One point which applies throughout the present work needs stressing at this stage. The restriction of our theory to small mutations implies that we are concerned with *local* geometric properties near to the singular strategy—that is with the region near the tip of the singular TIP.

For situations where f' is positive, it follows that the TIPs have their tips at the upper right corner; feasible parameter pairs (y_1, y_2)—consistent with the trade-off (5)—then lie below and to the left of the tip or above and to the right. However, the second set of points can be omitted since they are generated below and to the left in TIPs with upper right corners further up the trade-off curve. An identical argument for $f' < 0$ allows us to omit one set of points, and only consider TIPs containing feasible parameters that lie below and to the right of the tip.

There are four possible forms that the singular TIP can take. This follows since from (1) and (2) (applying (3)), we have as a special case of a general result

$$F_1(.., .., .., ..)|_* = \left.\frac{\partial s_x(y)}{\partial y_2}\right|_* = -\left.\frac{\partial s_y(x)}{\partial y_2}\right|_*. \tag{16}$$

Suppose first F_1 is positive (which it transpires is the case in Fig. 3), then as y_2 increases (as we move vertically up the TIP), $s_x(y)$ increases and is therefore positive above the curve f_1. Correspondingly from (16), $s_y(x)$ will decrease and hence be positive below the curve f_2. Given these results relating to changes with respect to y_2, the parallel results for changes with respect to y_1 are fixed by the identity

$$F_1(f_1(x_1,y_1),y_1,f(x_1),x_1)|_* f'(x_1^*) + F_2(f_1(x_1,y_1),y_1,f(x_1),x_1)|_* = 0, \quad (17)$$

which comes from differentiating (10) with respect to y_1 (see Appendix A (A.3)) and using the common tangent property of the three curves established above at (13). Thus when $s_x(y)$ is positive above the curve f_1, for $f'>0$, it is also positive to the left of this curve and, for $f'<0$, it is positive to the right. Similarly $s_y(x)$ positive below f_2 implies positivity to the right for $f'>0$, and to the left for $f'<0$. (These results use the analogue of (16) for y_1.) If we now suppose that F_1 is negative we obtain exactly the opposite results to the above. To move from 2 cases to 4 we have only to note that in each of the above cases the invasion properties will change depending on whether f_1 is locally above or below f_2 near the tip of the singular TIP, this depends on the relative curvatures of f_1 and f_2 since their gradients are identical. We thus have 4 cases. We do stress that although we only plot the TIPs in each case for f' being positive, the method, and hence the results, are independent of the sign of f' and apply for both $f'>0$ and $f'<0$; hence there are only 4 cases and not 8.

In order to begin our investigation into the evolutionary properties of TIPs, we shall study one particular form of the four main types. This will be the case—Case 1— where at the tip the curvature of f_1 is less than the curvature of f_2, and where $F_1>0$. Once the results are calculated for this particular singular TIP, the results for the other three can be easily found by appropriately changing the signs in inequalities found below. This particular TIP has the form as seen in Fig. 3. This TIP can be easily split into three regions, separated by the invasion boundaries, defining where each strategy can invade.

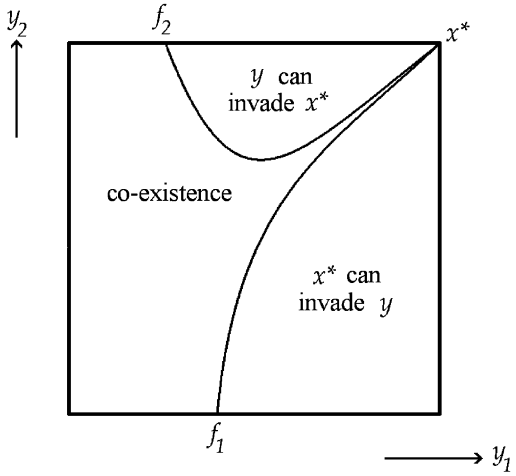

Fig. 3. A singular TIP for Case 1 (taking $f'>0$) in which the curvature at the origin of f_1 is less than that of f_2 and the fitness gradient at the origin for y invading x is positive. The figure shows which strain can invade the other if the feasible mutations (defined by the trade-off curve) occur in the delineated regions of the figure.

4. The geometric characterization of the singularity

Fig. 3 is as yet not fully developed as a TIP—the trade-off curve has not been included. We expect different types of evolutionary singularity to correspond to different completed—that is trade-off included—singular TIPs. We show that this is the case in what follows. We proceed by introducing the standard properties (evolutionary unbeatable strategy (EUS), spreading, convergence stability and MI) of such singularities and arguing *directly* from their definitions to corresponding geometric conditions on the singular TIP involving curvatures of the invasion boundaries and trade-off at the tip. We stress that our arguments are direct geometric ones—we make no use of the standard derivative conditions of adaptive dynamics (Geritz et al., 1997, 1998; Metz et al., 1996). We turn to the question of the equivalence of the two methods later.

We proceed by discussing the standard properties of evolutionary singularities in turn.

4.1. Evolutionary unbeatable strategy

The singular strategy x^* is (locally) an EUS if and only if there is no other (mutant) strategy that can invade x^*. (Our use of EUS is identical with the more standard ESS.)

In terms of TIPs, we can say that if and only if the trade-off curve enters the singular TIP in the region where $s_{x^*}(y)<0$, will it be the case that all feasible alternative strategies will have negative fitness making the strategy x^* an EUS. On the TIP of Fig. 3, the region $s_{x^*}(y)<0$ is below the invasion boundary f_1. As the gradients of the invasion boundaries equal that of the trade-off at the tip on the singular TIP, then to be EUS, is equivalent to satisfying the curvature condition

$$f''(x_1^*) < \left.\frac{\partial^2 f_1}{\partial y_1^2}\right|_* . \quad (18)$$

Clearly when (18) is reversed the trade-off enters the TIP above the invasion boundary f_1, where $s_{x^*}(y)>0$ and the singular strategy can be invaded by mutants y in the neighbourhood of x^*, which is equivalent to x^* being not EUS.

4.2. Spreading

A singular strategy, x^*, can *spread* (SPR), i.e. invade a nearby population y, if and only if $s_y(x^*)>0$ for all $y\neq x^*$. (In Apaloo (1977) the term neighbourhood invader strategy (NIS) is used in this context.)

On a TIP, this relates to the invasion boundary f_2. For the given strategy x^*, if and only if the trade-off curve enters the TIP in a region where $s_y(x^*)>0$, is it the case that the singular strategy can invade strategies $y\neq x^*$ making it SPR. This implies that x^* can spread into other populations if rare itself. In the TIP of Fig. 3, the fitness function $s_y(x^*)$ is positive below the curve f_2, and therefore x^* is SPR if and only if the trade-off curve lies in this region. Thus to be SPR is equivalent to the curvature condition

$$f''(x_1^*)<\left.\frac{\partial^2 f_2}{\partial y_1^2}\right|_*. \tag{19}$$

Clearly when (19) is reversed, the trade-off curve enters above f_2, the strategy y always wins, we have $s_y(x^*)<0$, and therefore the singular strategy cannot invade a strategy in the neighbourhood of x^*, and therefore it is not SPR. (Actually the upper quadrant of the TIP is needed for $y>x^*$. But this is included in (19) since we are working locally.)

4.3. Convergence stable

For the singularity to be *convergence stable* (CS), x must be susceptible to invasion by mutant strategies closer to the singularity, but not by ones that are further away. In this way the population will evolve towards the singularity.

In order to study this on the singular TIP, we must begin by looking at the TIPs either side of the singularity. For $x\neq x^*$, although all three curves have equal values at the tip of the TIP, the gradient of the trade-off curve differs from that of the invasion boundaries. Therefore the trade-off curve enters the TIP in a $(y_1<x_1)$ region which is determined entirely by comparing $f'(x_1)$ and the common gradient of the invasion curves at x. Furthermore this must be either in a region where y can invade x or x can invade y and, moreover, for $y_1>x_1$ these results are reversed. For Fig. 3 applied with tips near to x^*, y wins for $y_1<x_1$ if $f'(x_1)-\partial f_1/\partial y_1|_{y=x}$ is negative, whilst x wins for $y_1<x_1$ if $f'(x_1)-\partial f_1/\partial y_1|_{y=x}$ is positive. Noting that the above difference is zero at the singularity, for CS we want the former result to apply for $x_1^*<x_1$ and the latter for $x_1<x_1^*$. Thus, since we are working locally, we deduce that CS is equivalent to the condition

$$\left.\frac{\mathrm{d}}{\mathrm{d}x_1}\left(f'(x_1)-\left.\frac{\partial f_1}{\partial y_1}\right|_{y=x}\right)\right|_*<0. \tag{20}$$

We can simplify (20) using the second order derivatives of (10) and (11) given in the Appendix A. We evaluate these at the singularity and take $F_1|_*\neq 0$. From (A.5), (A.6) and (A.7), using (4), we have

$$\left.\frac{\partial^2 f_2}{\partial y_1^2}\right|_* - \left.\frac{\partial^2 f_1}{\partial y_1^2}\right|_* = 2\left.\frac{\partial^2 f_1}{\partial x_1\partial y_1}\right|_*. \tag{21}$$

We can now say from (20) and (21) that an equivalent condition for the singular strategy to be CS, is the requirement that the inequality

$$f''(x_1^*)<\frac{1}{2}\left(\left.\frac{\partial^2 f_1}{\partial y_1^2}\right|_{x_1^*}+\left.\frac{\partial^2 f_2}{\partial y_1^2}\right|_{x_1^*}\right). \tag{22}$$

is satisfied, i.e. the curvature of the trade-off at the tip of the singular TIP must be less than the mean curvature of the invasion boundaries.

This result could easily be found using the same relation between the trade-off curve and the second invasion boundary f_2. This route to the CS condition is symmetric to the way found above, as it can be found from (A.7) and (A.8) that:

$$\left.\frac{\partial^2 f_1}{\partial x_1\partial y_1}\right|_* + \left.\frac{\partial^2 f_2}{\partial x_1\partial y_1}\right|_* = 0. \tag{23}$$

4.4. Mutual invadability

If and only if, close to the singularity, there exist two distinct strategies x and y which give rise to a situation where $s_x(y)>0$ and $s_y(x)>0$, is it the case that both strategies when initially rare can invade the other. In such circumstances both strategies are protected from extinction. This gives rise to MI.

We consider TIPs, with tip at $x_1=x_1^*+h$, where h is a small positive constant. (Very little needs changing for h small and negative but this is less convenient since the quadrant above the tip is likely to need illustration.) On our TIPs MI is shown by a section of the trade-off curve passing through a region where both x and y can invade, i.e. where $s_x(y)>0$ and $s_y(x)>0$. As mentioned earlier, away from the singular TIP, even in the linear approximation the trade-off curve enters the TIP in a region where either x wins or y wins, but not in the coexistence region. In principle therefore the trade-off curve may cross neither, one or both of the invasion boundaries away from x_1 (where it must cross) in the neighbourhood of x^*. We aim to show that there are always such crossings since this is necessary for MI. We take $\tilde{y}_i$ to represent the value of y_1 for which the trade-off crosses f_1 for $i=1$ and f_2 for $i=2$; here $\tilde{y}_i=x_1^*+h-k_i$, where k_i represents the distance from the tip to where the trade-off crosses f_1 and f_2 (for $i=1,2$, respectively). Hence a positive k_i represents a crossing at $\tilde{y}_i<x_1$, and a negative k_i at $\tilde{y}_i>x_1$. Calculating the

Taylor series, truncated at order 2, gives

$$f(x_1^*+h-k_i)=f(x_1^*)+(h-k_i)f'(x_1^*)+\frac{1}{2}(h-k_i)^2f''(x_1^*)\quad\text{for } i=1,2 \tag{24}$$

for the trade-off, and for the invasion boundaries

$$\begin{aligned}f_i(x_1^*+h,x_1^*+h-k_i)&=f_i(x_1^*,x_1^*)+(h-k_i)\left.\frac{\partial f_i}{\partial y_1}\right|_*\\&\quad+\frac{1}{2}\left(h^2\left.\frac{\partial^2 f_i}{\partial x_1^2}\right|_*+2h(h-k_i)\left.\frac{\partial^2 f_i}{\partial x_1\partial y_1}\right|_*\right.\\&\quad\left.+(h-k_i)^2\left.\frac{\partial^2 f_i}{\partial y_1^2}\right|_*\right).\end{aligned} \tag{25}$$

An obvious intersection is where all three lines cross at the tip, i.e. when $k_i=0$ (hence $\tilde{y}_i=x_1$) for $i=1,2$. This produces the result

$$f''(x_1^*)=\left.\frac{\partial^2 f_i}{\partial x_1^2}\right|_*+2\left.\frac{\partial^2 f_i}{\partial x_1\partial y_1}\right|_*+\left.\frac{\partial^2 f_i}{\partial y_1^2}\right|_*. \tag{26}$$

Using this, and the result found in (21), we can show that there are always crossing points and these occur when

$$\begin{aligned}k_1&=h\left(1+\frac{f''(x_1^*)-\left.\frac{\partial^2 f_2}{\partial y_1^2}\right|_*}{f''(x_1^*)-\left.\frac{\partial^2 f_1}{\partial y_1^2}\right|_*}\right),\\k_2&=h\left(1+\frac{f''(x_1^*)-\left.\frac{\partial^2 f_1}{\partial y_1^2}\right|_*}{f''(x_1^*)-\left.\frac{\partial^2 f_2}{\partial y_1^2}\right|_*}\right).\end{aligned} \tag{27}$$

Taking h to be a sufficiently small positive constant will ensure the crossings are close to the tip of the TIP.

It is actually possible to obtain more details about the crossings as follows. The values y_1 for where a crossing takes place can be split into 3 regions, $\tilde{y}_i>x_1$, $x_1^*<\tilde{y}_i<x_1$ and $\tilde{y}_i<x_1^*$. Firstly, we look at a crossing of f with f_1 occurring at $\tilde{y}_1>x_1$. For simplicity, we let $A=f''(x_1^*)-\left.\frac{\partial^2 f_2}{\partial y_1^2}\right|_*$ and $B=f''(x_1^*)-\left.\frac{\partial^2 f_1}{\partial y_1^2}\right|_*$. This produces

$$\begin{aligned}\tilde{y}_1>x_1&\Leftrightarrow k_1<0\Leftrightarrow\frac{A}{B}<-1\Leftrightarrow-1<\frac{B}{A}<0\\&\Leftrightarrow 0<k_2<h\Leftrightarrow x_1^*<\tilde{y}_2<x_1.\end{aligned} \tag{28}$$

Thus, if a crossing of one invasion boundary occurs at $\tilde{y}_1>x_1$, then a crossing of second invasion boundary occurs between the tip and the singularity. The second case, when the crossing between f and f_1 occurs in the region $x_1^*<\tilde{y}_1<x_1$, corresponding to the other crossing occurring for $\tilde{y}_2>x_1$; which can be seen by following through the above argument in reverse. Thirdly, if a crossing occurs for $\tilde{y}_1<x_1^*$, then

$$\begin{aligned}\tilde{y}_1<x_1^*&\Leftrightarrow k_1>h\Leftrightarrow\frac{A}{B}>0\Leftrightarrow\frac{B}{A}>0\\&\Leftrightarrow k_2>h\Leftrightarrow\tilde{y}_2<x_1^*.\end{aligned} \tag{29}$$

Thus if the trade-off crosses f_1 at $\tilde{y}_1<x_1^*$, then it must also cross f_2 at $\tilde{y}_2<x_1^*$. Combining these and using symmetry properties, we can state that the trade-off curve must cross at least one of the invasion boundaries at $\tilde{y}_i<x_1$.

We saw earlier that above the singularity, at the tip of a TIP the trade-off will either enter a region where x can invade y or y can invade x. However, we now know that the trade-off curve will always cross both invasion boundaries (and at least one at a point $y_1<x_1$), and therefore in the case of Fig. 3 it must pass into the region where the two strategies can coexist. Our arguments above about the intersections apply generally. Hence, without restriction to the case of Fig. 3, we can conclude that, if and only if there exists a region on the singular TIP where both $s_x(y)>0$ and $s_y(x)>0$, then there will exist mutually invadable strategies in the neighbourhood of the singular one. (We can specify the singular TIP in this condition since the existence of the required region is shared generically by continuity by neighbouring TIPs.)

4.5. Summary of properties

We can now summarize in Table 1 which properties occur based on the curvatures of f, f_1 and f_2 at the tip of the singular TIP. Labelling the appropriate regions with these properties, we get the TIP in Fig. 4. The dashed line represents the mean curvature of the invasion boundaries at the tip.

The final column in Table 1 indicates the corresponding evolutionary outcome. The two important properties, EUS and CS, combine to give one of four possible scenarios. The singularity is an *evolutionary attractor* if and only if the population, being CS, evolves towards x^*, which is EUS (so an alternative term is 'a convergence stable EUS/ESS'). It is an *evolutionary*

Table 1
Evolutionary properties of x^*, where $F_1|_*>0$ and $f_2''>f_1''$. Here $f''=f''(x^*)$, $f_1''=\left.\frac{\partial^2 f_1}{\partial y_1^2}\right|_*$ and $f_2''=\left.\frac{\partial^2 f_2}{\partial y_1^2}\right|_*$

Trade-off curvature	EUS	CS	SPR	MI	Type
$f''>f_2''$	×	×	×	√	Repellor
$f_2''>f''>\frac{1}{2}(f_1''+f_2'')$	×	×	√	√	Repellor
$\frac{1}{2}(f_1''+f_2'')>f''>f_1''$	×	√	√	√	Branching point
$f_1''>f''$	√	√	√	√	Attractor

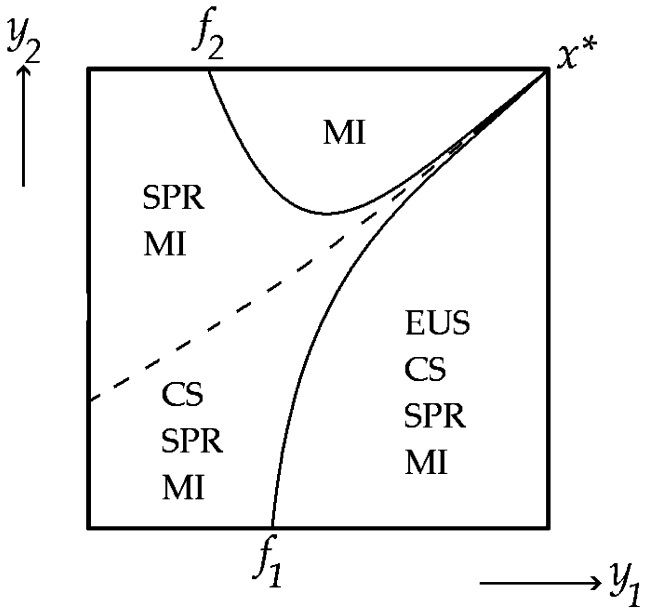

Fig. 4. A singular TIP for the case in which the curvature at the origin of f_1 is less than that of f_2 and the fitness gradient at the origin for y invading x is positive. The figure shows the properties enjoyed by the singular strain (at the origin) if the feasible mutations (defined by the trade-off curve) occur in the delineated regions of the figure.

repellor if and only if the strategy always evolves away from the singular strategy, which is not EUS. The singularity is a '*Garden of Eden*' point if and only if the strategy always evolves away from the singular strategy, which is itself EUS. Most significantly, x^* is an *evolutionary branching point* (Geritz et al., 1998) if and only if the population evolves towards this strategy, which however is not EUS.

5. The other three cases of singular TIP

For reference, the other three types of singular TIPs, are shown in Fig. 5. Again (for diagrammatic purposes) we only plot figures where $f'>0$; the results below however, apply for both f' being positive or negative.

The TIP in Case 2 represents the situation where $F_1|_*>0$ and the curvature of f_1 is greater than that of f_2 at the singularity. Cases 3 and 4 are for $F_1|_*<0$, where the singular curvature of f_2 is greater than that of f_1 in Case 3 and less than it in Case 4.

Case 2: All the above work has assumed that at the tip the curvature of f_2 is greater than that of f_1. However if we reverse the situation, so that the curvature of f_1 is greater than that of f_2, but keep $F_1|_*>0$, then a straightforward modification of the method gives the results of Table 2. We see that the curvature conditions have now changed not in themselves but in their realization on the TIP. The most significant result concerns the fact that, in the centre region in Fig. 5, we now have a contingent situation concerning the strategies. In the upper part of this region, the singularity is EUS but not CS, implying that we have the Garden of Eden scenario.

Case 3: $F_1|_*<0$, and the tip curvature of f_2 greater than that of f_1. This causes a reversal in basic inequalities presented for Case 1. It gives rise to the results in Table 3 and yields the evolutionary scenario of Garden of Eden due to the contingent region in the centre.

Case 4: The final case again involves $F_1|_*<0$, however the tip curvatures of the invasion boundaries are now reversed. Here the curvature of f_2 is now less than the curvature of f_1 at the singularity. This modifies the results in Case 3 in much the same way as Case 2 modifies Case 1 and produces the results in Table 4. This again shows an area where the two strategies, x and y, can coexist, and hence the singularity is MI. This again leads to the possibility of branching in the centre region of the singular TIP.

6. The relationship with the standard derivative conditions of adaptive dynamics

So far we have found by direct geometric argument curvature conditions for the evolutionary properties. But how is our work related to an approach based on the standard derivative conditions of adaptive dynamics (in the presence of trade-offs)? These are shown in Table 5 (Geritz et al., 1997, 1998). In this section, we show formally that the two approaches are equivalent. Thus using the present approach the standard derivative conditions can be derived. Alternatively, starting from these conditions the curvature conditions can be extracted (but in a manner which is not based directly on the geometry of the trade-off).

The conditions of Table 5 all use the single fitness function $s_x(y)$ via its second derivative with respect to the mutant strategy y_1 and its second derivative with respect to the resident strategy x_1 (both evaluated at the singularity). We use the result $\partial^2 s_x(y)/\partial x_1^2|_* = \partial^2 s_y(x)/\partial y_1^2|_*$ to take all the derivation with respect to y_1.

To show directly the equivalence between our results derived geometrically and the standard adaptive dynamics conditions, we work with the case(s) where F_1 is positive. Our results still apply in the case(s) where F_1 is negative, due to a 'flipping of conditions' that were seen in the previous section containing the results for the other cases.

Concerning the fitness gradient from adaptive dynamics, by subtracting the first derivative of (10) with respect to y_1, (A.3), from the first derivative of $s_x(y)$ with respect to y_1, (A.9), and evaluating the result at the

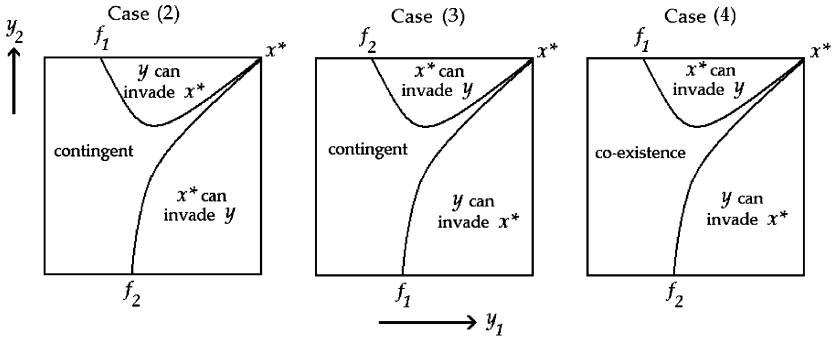

Fig. 5. Singular TIPs—modifications of Fig. 3—corresponding to the remaining Cases 2–4 of curvatures and fitness gradients explained in the text (for $f'>0$).

Table 2
Properties for $F_1|_*>0$ and $f_1''>f_2''$, where $f''=f''(x^*)$, $f_1''=\frac{\partial^2 f_1}{\partial y_1^2}\Big|_*$ and $f_2''=\frac{\partial^2 f_2}{\partial y_1^2}\Big|_*$

Trade-off curvature	EUS	CS	SPR	MI	Type
$f''>f_1''$	×	×	×	×	Repellor
$f_1''>f''>\frac{1}{2}(f_1''+f_2'')$	√	×	×	×	Garden of Eden
$\frac{1}{2}(f_1''+f_2'')>f''>f_2''$	√	√	×	×	Attractor
$f_2''>f''$	√	√	√	×	Attractor

Table 3
Properties for $F_1|_*<0$ and $f_2''>f_1''$, where $f''=f''(x^*)$, $f_1''=\frac{\partial^2 f_1}{\partial y_1^2}\Big|_*$ and $f_2''=\frac{\partial^2 f_2}{\partial y_1^2}\Big|_*$

Trade-off curvature	EUS	CS	SPR	MI	Type
$f''>f_2''$	√	√	√	×	Attractor
$f_2''>f''>\frac{1}{2}(f_1''+f_2'')$	√	√	×	×	Attractor
$\frac{1}{2}(f_1''+f_2'')>f''>f_1''$	√	×	×	×	Garden of Eden
$f_1''>f''$	×	×	×	×	Repellor

Table 4
Properties for $F_1|_*<0$ and $f_1''>f_2''$, where $f''=f''(x^*)$, $f_1''=\frac{\partial^2 f_1}{\partial y_1^2}\Big|_*$ and $f_2''=\frac{\partial^2 f_2}{\partial y_1^2}\Big|_*$

Trade-off curvature	EUS	CS	SPR	MI	Type
$f''>f_1''$	√	√	√	√	Attractor
$f_1''>f''>\frac{1}{2}(f_1''+f_2'')$	×	√	√	√	Branching point
$\frac{1}{2}(f_1''+f_2'')>f''>f_2''$	×	×	√	√	Repellor
$f_2''>f''$	×	×	×	√	Repellor

singularity we find

$$f'(x_1^*)=\frac{\partial f_1}{\partial y_1}\Big|_* \Leftrightarrow \frac{\partial s_x(y)}{\partial y_1}\Big|_*=0. \tag{30}$$

Table 5
Properties of x^*, where $s_{xx}=\frac{\partial^2 s_x(y)}{\partial x_1^2}\Big|_*$ and $s_{yy}=\frac{\partial^2 s_x(y)}{\partial y_1^2}\Big|_*$

Property	Condition
EUS	$s_{yy}<0$
CS	$s_{xx}-s_{yy}>0$
Spreading	$s_{xx}>0$
Mutually invadable	$s_{xx}+s_{yy}>0$

So our tangential condition for the location of the singularity is equivalent to the standard result (Geritz et al., 1997, 1998) concerning zero fitness gradient.

For the first property, EUS, by substituting the second derivative of (10) recorded at (A.5), into the second derivative of $s_x(y)$ at (A.11), we find

$$\text{EUS} \Leftrightarrow f''(x_1^*)<\frac{\partial^2 f_1}{\partial y_1^2}\Big|_* \Leftrightarrow \frac{\partial^2 s_x(y)}{\partial y_1^2}\Big|_*<0. \tag{31}$$

This is identical to the standard condition for EUS in Table 5.

A similar method can be used to for SPR. Now by substituting the second derivative of (11) recorded at (A.6), into the second derivative of $s_y(x)$ at (A.12), we find

$$\text{SPR} \Leftrightarrow f''(x_1^*)<\frac{\partial^2 f_2}{\partial y_1^2}\Big|_{x_1^*} \Leftrightarrow \frac{\partial^2 s_x(y)}{\partial x_1^2}\Big|_{x_1^*}>0, \tag{32}$$

which again matches the standard result from adaptive dynamics.

For the CS property, we require to substitute the difference in the second derivatives of (11) and (10) recorded in (A.6) and (A.5), into the difference in the second derivatives of $s_y(x)$ and $s_x(y)$, at (A.12) and (A.11). This produces

$$\begin{aligned}\text{CS} &\Leftrightarrow f''(x_1^*)<\frac{1}{2}\left(\frac{\partial^2 f_1}{\partial y_1^2}\Big|_*+\frac{\partial^2 f_2}{\partial y_1^2}\Big|_*\right)\\ &\Leftrightarrow \frac{\partial^2 s_x(y)}{\partial x_1^2}\Big|_*-\frac{\partial^2 s_x(y)}{\partial y_1^2}\Big|_*>0.\end{aligned} \tag{33}$$

This is again equivalent to the standard condition in the table above.

For the final evolutionary property, MI, the argument is similar to that for the CS condition above. We must substitute the sum of the second derivatives of (10) and (11), given at (A.5) and (A.6), into the sum of the second derivatives of $s_x(y)$ and $s_y(x)$, given at (A.11) and (A.12). This gives

$$\begin{aligned}\mathrm{MI} &\Leftrightarrow \left.\frac{\partial^2 f_1}{\partial y_1^2}\right|_* < \left.\frac{\partial^2 f_2}{\partial y_1^2}\right|_* \\ &\Leftrightarrow \left.\frac{\partial^2 s_x(y)}{\partial x_1^2}\right|_* + \left.\frac{\partial^2 s_x(y)}{\partial y_1^2}\right|_* > 0, \end{aligned} \tag{34}$$

which is identical to the standard MI condition in Table 5.

We can summarize the results of this section by saying that the TIP curvature conditions we have derived are equivalent (in the presence of trade-offs) to the standard derivative conditions of adaptive dynamics.

7. Example

In this section, we shall provide an illustrative application of our theory. We shall consider prey evolution in a predator–prey model (with an implicit carrying capacity) and a Holling's (1959) Type II Functional Response; we shall take the predator to be fixed. Thus our system will consist of two prey strains, x and y and a single predator strain. These have population densities given by (N_x, N_y, P) respectively. The model therefore takes the form

$$\frac{\mathrm{d}N_x}{\mathrm{d}t} = N_x\left(r_x - q(N_x+N_y) - \frac{k_x P}{N_x+N_y+D}\right), \tag{35}$$

$$\frac{\mathrm{d}N_y}{\mathrm{d}t} = N_y\left(r_y - q(N_x+N_y) - \frac{k_y P}{N_x+N_y+D}\right), \tag{36}$$

$$\frac{\mathrm{d}P}{\mathrm{d}t} = P\left(-b + \frac{\beta k_x N_x}{N_x+N_y+D} + \frac{\beta k_y N_y}{N_x+N_y+D}\right). \tag{37}$$

Here, r_i is the intrinsic growth rate of prey strain i, q is a competition coefficient, incorporating the carrying capacity implicitly and k_i is the maximum rate of predation on prey strain i. Also, b is the death rate of the predator, β is the growth rate (conversion rate) of the predator due to predation, and D is the level of prey population density after which predation capability begins to saturate. All the parameters affect the population densities of both prey strains equally with the exception of r and k. A trade-off is introduced between these parameters in such a way that a reduction in predation rate is achieved at a cost of a lower birth rate, i.e. $r_i = f(k_i)$, with f' positive. This leads to TIPs of the form shown in the examples above, where the tip of the TIP is located in the top-right corner as $f'(k_i) > 0$. In order to make the correspondence with general theory more easily, we shall re-label the parameters k_x and k_y as x_1 and y_1, and r_x and r_y as x_2 and y_2.

There are two fitness functions that we need, one, $s_x(y)$, where the x strain is the resident and y is the invading (mutant) strain, and one, $s_y(x)$, where the roles are reversed. We find directly from per capita growth rates in (35) and (36)—the terms in brackets—that

$$s_x(y) = y_2 - \frac{y_1}{x_1}\left(x_2 - \frac{qbD}{\beta x_1 - b}\right) - \frac{qbD}{\beta x_1 - b}, \tag{38}$$

$$s_y(x) = x_2 - \frac{x_1}{y_1}\left(y_2 - \frac{qbD}{\beta y_1 - b}\right) - \frac{qbD}{\beta y_1 - b}. \tag{39}$$

In establishing (38) we set, in the per capita growth rate of (36), the densities of the resident prey strain x and the predator at the equilibrium values obtained from (35) and (37) in the absence of the prey strain y. (We assume that the equilibrium is stable.) Eq. (39) is obtained in a symmetrical fashion. Eqs. (38) and (39) are concrete forms of (1) and (2). The next step concerns calculating the two invasion boundaries f_1 and f_2. Along these boundaries, the strains have zero fitness. Setting the fitness functions to zero and solving for y_2, gives

$$y_2 = \phi_1(x_2, x_1, y_1) = \frac{y_1}{x_1}\left(x_2 - \frac{qbD}{\beta x_1 - b}\right) + \frac{qbD}{\beta x_1 - b}, \tag{40}$$

$$y_2 = \phi_2(x_2, x_1, y_1) = \frac{y_1}{x_1}\left(x_2 - \frac{qbD}{\beta y_1 - b}\right) + \frac{qbD}{\beta y_1 - b}, \tag{41}$$

which are concrete forms of (8) and (9).

The third curve, the trade-off curve, we take to have the explicit form of

$$y_2 = f(y_1) = a y_1^2 + 5y_1 + a + 1. \tag{42}$$

For technical reasons, we take a to be in the range $-1 \leqslant a \leqslant 1$. This same form is used for x_2, i.e. $x_2 = a x_1^2 + 5x_1 + a + 1$ and using this result in (40) and (41) provides the f_1 and f_2 of (8) and (9).

Now, the location of any singularity can be calculated by solving, for x_1, the equation which expresses the fact that the trade-off curve is tangential to the invasion boundaries when $y_1 = x_1$. Taking the numerical values for the parameters of $q = b = 1$, $D = 10.5$ and $\beta = 11.5$, results in a solution at $x_1^* = 1$ (We choose parameter values such that the point equilibrium used in (40) and (41) is stable.). The curvatures of the trade-off curve (which we have arranged to vary conveniently with a) and the two invasion boundaries, at this singularity, are given by

$$f''(x_1^*) = 2a, \quad \left.\frac{\partial^2 f_1}{\partial y_1^2}\right|_* = 0, \quad \left.\frac{\partial^2 f_2}{\partial y_1^2}\right|_* = \frac{46}{21}. \tag{43}$$

From the two invasion boundaries, we get that the mean curvature is 23/21. Therefore, we can break the range of a into three regions, each representing an evolutionary scenario, giving

$$\begin{aligned} &\text{Evolutionary Attractor:} && -1<a<0,\\ &\text{Evolutionary Branching:} && 0<a<\tfrac{23}{42},\\ &\text{Evolutionary Repellor:} && \tfrac{23}{42}<a<1. \end{aligned} \tag{44}$$

(Since, $F_1>0$ and $\left.\frac{\partial^2 f_2}{\partial y_1^2}\right|_* > \left.\frac{\partial^2 f_1}{\partial y_1^2}\right|_*$, we are in Case 1 and Table 1 applies.)

Using these, we can plot three TIPs for relevant values of a, one for each scenario. Fig. 6 displays the TIPs, and corresponding computer simulations of the evolutionary dynamics, for $a=-0.3$ verifying that the singularity is indeed an attractor, a branching point for the value $a=0.3$ and a repellor for $a=0.8$. (See Bowers et al. (2003) for details of the simulation process.)

The major point of our example is to illustrate the results in Table 1. For this purpose concentrating on one singularity and fixing it at $x_1^*=1$ suffices. However, we

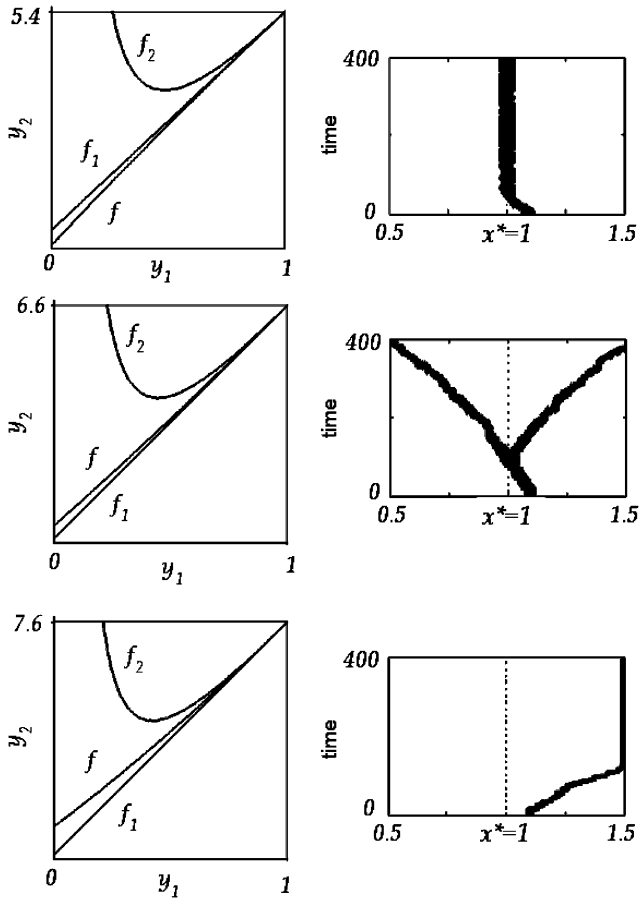

Fig. 6. TIPs and corresponding simulations for the example with $a=-0.3$; 0.3; 0.8. The simulations verify/illustrate the classification of Fig. 4 and Table 1. Trade-offs of different curvatures yield an evolutionary attractor, an evolutionary branching point and an evolutionary repellor respectively as the curvature increases.

can analyse the model more fully so as to reveal an underlying reason for the change in CS behaviour at $a=23/42$. Calculating where the trade-off curve is tangential to the invasion boundaries (at the tip) reveals a second singularity $x^\dagger$, where

$$x_1^\dagger = \frac{-21a+\sqrt{625a^2+2116a}}{46a}. \tag{45}$$

The curvatures of the trade-off curve and the invasion boundary f_1 remain unchanged; however the curvature of f_2 now becomes

$$\left.\frac{\partial^2 f_2}{\partial y_1^2}\right|_\dagger = \frac{2}{x^\dagger}\left(\frac{120.75}{(11.5x^\dagger-1)^2}\right). \tag{46}$$

The first comment that should be made is that this singularity is only biologically feasible for $a>0$, which implies that $x^\dagger$ can never be EUS. However, concerning convergence stability, this singularity is such that for a just less than 23/42, it is not CS which means that it is an evolutionary repellor, whilst for a just greater than 23/42, $x^\dagger$ is CS which means that it is an evolutionary branching point. The two singularities cross each other when $a=23/42$ in a (degenerate) transcritical bifurcation. (There is a third singularity but it is not biologically feasible.)

8. Discussion

The main thrust of this paper has been to establish a geometric approach to adaptive evolution subject to trade-offs. Our approach is independent of the usual techniques of adaptive dynamics involving partial derivatives of the fitness function. However, it utilizes all the assumptions developed in the standard approach (Dieckmann and Law, 1996; Geritz et al., 1997, 1998; Metz et al., 1996) and we have shown the two approaches to be equivalent (in the presence of trade-offs). Our principal results are really those presented algebraically in Tables 1–4 corresponding to Cases 1–4 as explained above. More striking, however, is the geometric representation of these in Fig. 4 (and its equivalent for the other cases).

In the Case 1 shown in Fig. 3 (Table 1), we see that a condition on the trade-off curve of intermediate curvature is needed for the singularity to be a branching point. A similar condition is also needed in Case 4 (Fig. 5 and Table 4). This has possible implications for understanding polymorphism and speciation (Bowers and White, 2002; Geritz et al., 1997; Geritz et al., 1998; Metz et al., 1996; White and Bowers, 2004). The more detailed investigation of these conditions is one of the many areas of future research which the present approach suggests. We give one example to illustrate the possibilities.

We can show that, in the case where there is no interspecific parameter dependence in the population dynamics, that given $F_1|_* \neq 0$, we have

$$\left.\frac{\partial^2 f_1}{\partial y_1^2}\right|_* = \left.\frac{\partial^2 f_2}{\partial y_1^2}\right|_*. \tag{47}$$

Hence the curvatures of the two invasion boundaries are equal at the singularity, and hence identical with the mean curvature. This is equivalent to there being no coexistence (or contingent) region in the TIPs. Therefore, the conditions for EUS, CS and SPR are identical; there is no region of intermediate curvature and no possibility of branching points (or Garden of Eden points). This agrees with a result obtained by Bowers and White (2002) in the restricted context of Lotka–Volterra systems and relates to the work of Metz et al. (1996) and Meszéna et al. (2001) on optimization.

Another issue of interest is the connection between the classification of singularities presented in Figs. 3 and 5 (Tables 1–4) and the classification provided by the eight-fold way connected with PIPs (Geritz et al., 1997, 1998; Metz et al., 1996). The path the trade-off curve takes as the curvature increases can be represented on the eight-fold graph of PIPs. By re-labelling each of the 8 PIPs on this by its properties, we can track how the PIPs change as $f''(x^*)$ increases and moves through each of four regions, and how the curvature of each invasion boundary and the mean of these curvatures are represented by an axis or main diagonal on the eight-fold graph. This is seen for Case 1 (Fig. 3 and Table 1) in Fig. 7; the arrow represents the direction of travel as $f''(x^*)$ increases. Notice that the path passes through the branching segment. For Case 2 (Fig. 5 and Table 2), on the eight-fold plot in Fig. 7, the path again starts in the same position, in the Southeast, but now travels in a clockwise direction. For Case 3 (Fig. 5 and Table 3), on the eight-fold plot in Fig. 7, the path now starts in the Northwest position and travels in an anti-clockwise direction. Finally for Case 4 (Fig. 5 and Table 4), on the eight-fold plot in Fig. 7, the path again starts in the Northwest position, but now travels in a clockwise direction, again passing the branching segment. (A word of warning emerging from our analysis of the example is perhaps in order here. If Fig. 7 or Tables 1–4 are used in a context where singularities are followed as functions of a parameter, then changes in the CS behaviour can only occur via bifurcations involving the interaction of at least two singularities.)

We close this paper with some general observations about the usefulness of our approach in analysing evolutionary dynamics. Our starting point is the value of geometrical applications in both presenting and disseminating theory and making it more accessible for applications. For recent related work see Rueffler et al., 2004, De Mazancourt and Dieckmann, 2004. These

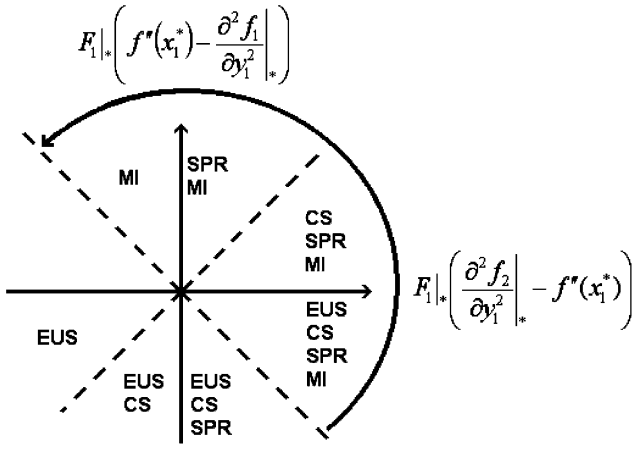

Fig. 7. The relationship between the classification of singularities derived here and the classification provided by the eight-fold way connected with PIPs is shown. The path the trade-off curve takes as its singular curvature increases is represented by the arrow on the eight-fold graph of PIPs. Each of the 8 types of PIP is represented by its properties and the figure shows how the PIP type changes as $f''(x_1^*)$ increases and so moves through each of four regions. The equality of the trade-off curvature with the curvature of each invasion boundary and with the mean of these curvatures is represented by an axis or main diagonal on the eight-fold graph. The diagram corresponds to Case 1 (Fig. 3 and Table 1).

authors develop their theory from the approach of Levins (1962) which is based on superimposing the trade-off onto fitness contours. This focuses attention on the contour which is tangential to the trade-off at the singular strategy and is an invasion boundary. Evolutionary behaviour can be inferred from the relative curvatures of the lines. Our approach is an extension of the reciprocal invasion plots used in Antonovics and Thrall (1994), Boots and Bowers (1999, 2004) and Bowers et al. (1994). Here, as we have shown, TIPs are constructed by adding the trade-off curve to the plots, the singular TIP is identified by a condition of mutual tangentiality and the evolutionary behaviour can be inferred from this using the relative curvatures of the trade-off and the two invasion boundaries. The behaviour can also be extracted in a straightforward manner from a visual inspection of the singular TIP.

As far as presentation and dissemination is concerned, we can make our point by referring to the sequence of figures in this article. In the case of TIPs, the geometric objects have immediate interpretations—the trade-off represents a constraint and the invasion curves are the boundaries between the regions where either strain as rare mutant can invade the other as resident. Thus the content of Fig. 1 is directly accessible. In a TIP one strain is fixed whilst the other varies. If we now allow the fixed strain also to vary—whilst accepting that it must lie on the trade-off curve—we obtain a 'bundle' of TIPs as in Fig. 2. Now we can appreciate the nature of

evolutionary singularity. Combining Fig. 2 with Fig. 3 we see that there is a dramatic evolutionary change as we move through the TIP in which all three curves are tangential—the 'winning' strain changes. Fig. 4 shows how the evolutionary properties—which determine the outcome of evolution—can be directly read off the singular TIP by observing which region of the singular TIP the trade-off enters as it curves away from the invasion boundaries.

As far as application is concerned, the direct connection between the position of the trade-off curve on the singular TIP and the evolutionary behaviour is of prime importance. This is illustrated by applications such as Fig. 6 which shows attractor, branching-point and repellor behaviour classified by TIPs and derived from simulations in full agreement. This example can be used to highlight other issues. According to (44), in the example, branching can only occur for trade-offs with positive curvature below a certain threshold. (Such trade-offs are described as corresponding to weakly accelerating costs in White and Bowers (2004).) Since the invasion boundary, (f_1), has zero curvature (Fig. 6), branching can never occur in this example for trade-offs with negative curvature (or equivalently decelerating costs). This can be seen directly from the TIP even when the trade-off curve itself is omitted. Thus an inspection of the TIP allows us to see immediately the shape of the trade-off curve required to produce particular evolutionary behaviour. This interpretation applies generally and highlights the usefulness of TIPs and the importance of trade-off shapes in determining evolutionary behaviour. For example, Fig. 4 shows that, when (f_1) has negative curvature, branching will be possible with sufficiently weakly decelerating costs. To summarize, with TIPs the effect of varying the trade-off can be discussed very efficiently on one diagram. This contrasts with how one would proceed with PIPs since the explicit nature of the trade-off is more deeply embedded there.

The benefits of an approach based on TIPs for both general theory and application are clear.

Appendix A

The equations displayed in this appendix deal with the derivatives of the fitness functions $s_x(y)$ and $s_y(x)$, and the derivatives of the functions in (10) and (11). They are used throughout the main text of this article and collected here for convenience. Recall that we have used the notation $F_i(..,..,..,..)$ to represent the derivative of F with respect to the ith parameter, where $i = 1, 2, 3, 4$. We assume the usual symmetry condition on mixed partial derivatives wherever convenient.

The first set of derivatives is those of Eqs. (10) and (11) differentiated with respect to x_1, and evaluated at the singularity. Using (3), we find

$$\left(F_1(f_1(x_1,y_1),y_1,f(x_1),x_1)\frac{\partial f_1}{\partial x_1} - F_1(f_1(x_1,y_1),y_1,f(x_1),x_1)f'(x_1) - F_2(f_1(x_1,y_1),y_1,f(x_1),x_1)\right)\Big|_* = 0 \tag{A.1}$$

and

$$\left(F_1(f(x_1),x_1,f_2(x_1,y_1),y_1)f'(x_1) - F_1(f(x_1),x_1,f_2(x_1,y_1),y_1)\frac{\partial f_2}{\partial x_1} + F_2(f(x_1),x_1,f_2(x_1,y_1),y_1)\right)\Big|_* = 0. \tag{A.2}$$

As an aside, we note that, since, as lists, the arguments of each occurrence of an F_i in (A.1) and (A.2) are identical at the tip of any TIP, the two quantities $\partial f_1/\partial x_1$ and $\partial f_2/\partial x_1$ are equal at the tip of the singular TIP.

Calculating the derivatives of these two Eqs. (10) and (11), but now with respect to y_1, we get

$$F_1(f_1(x_1,y_1),y_1,f(x_1),x_1)\frac{\partial f_1}{\partial y_1} + F_2(f_1(x_1,y_1),y_1,f(x_1),x_1) = 0, \tag{A.3}$$

$$F_3(f(x_1),x_1,f_2(x_1,y_1),y_1)\frac{\partial f_2}{\partial y_1} + F_4(f(x_1),x_1,f_2(x_1,y_1),y_1) = 0. \tag{A.4}$$

As an aside, we note that, for the reason given following (A.2), the two invasion curves have equal gradients $\partial f_1/\partial y_1$ and $\partial f_2/\partial y_1$ at the tip of any TIP. Calculating the derivatives of (A.3) and (A.4) with respect to y_1, and evaluating at x^*, gives

$$\left[F_{11}(f_1(x_1,y_1),y_1,f(x_1),x_1)\left(\frac{\partial f_1}{\partial y_1}\right)^2 + 2F_{12}(f_1(x_1,y_1),y_1,f(x_1),x_1)\frac{\partial f_1}{\partial y_1} + F_1(f_1(x_1,y_1),y_1,f(x_1),x_1)\frac{\partial^2 f_1}{\partial y_1^2} + F_{22}(f_1(x_1,y_1),y_1,f(x_1),x_1)\right]\Big|_* = 0 \tag{A.5}$$

and

$$\left[F_{33}(f(x_1),x_1,f_2(x_1,y_1),y_1)\left(\frac{\partial f_2}{\partial y_1}\right)^2 + 2F_{34}(f(x_1),x_1,f_2(x_1,y_1),y_1)\frac{\partial f_2}{\partial y_1} + F_3(f(x_1),x_1,f_2(x_1,y_1),y_1)\frac{\partial^2 f_2}{\partial y_1^2} + F_{44}(f(x_1),x_1,f_2(x_1,y_1),y_1)\right]\Big|_* = 0. \tag{A.6}$$

The derivatives of (A.3) and (A.4) with respect to x_1, again evaluated at the singularity, are also required. Hence using the result from (15), concerning $\partial f_i/\partial x|_*$, gives

$$\begin{aligned}\Big[&F_{13}(f_1(x_1,y_1),y_1,f(x_1),x_1)\frac{\partial f_1}{\partial y_1}f'(x_1)\\&+F_{14}(f_1(x_1,y_1),y_1,f(x_1),x_1)\frac{\partial f_1}{\partial y_1}\\&+F_1(f_1(x_1,y_1),y_1,f(x_1),x_1)\frac{\partial^2 f_1}{\partial x_1\partial y_1}\\&+F_{23}(f_1(x_1,y_1),y_1,f(x_1),x_1)f'(x_1)\\&+F_{24}(f_1(x_1,y_1),y_1,f(x_1),x_1)\Big]\Big|_*=0\end{aligned}\tag{A.7}$$

and

$$\begin{aligned}\Big[&F_{31}(f(x_1),x_1,f_2(x_1,y_1),y_1)\frac{\partial f_2}{\partial y_1}f'(x_1)\\&+F_{32}(f(x_1),x_1,f_2(x_1,y_1),y_1)\frac{\partial f_2}{\partial y_1}\\&+F_{41}(f(x_1),x_1,f_2(x_1,y_1),y_1)f'(x_1)\\&+F_{42}(f(x_1),x_1,f_2(x_1,y_1),y_1)\\&+F_3(f_2(x_1,y_1),y_1,f_2(x_1,y_1),y_1)\frac{\partial^2 f_2}{\partial x_1\partial y_1}\Big]\Big|_*=0.\end{aligned}\tag{A.8}$$

The final set of results required is the derivatives of the fitness functions $s_x(y)$ and $s_y(x)$ of (6) and (7) with respect to y_1. Calculating the first derivatives, we get

$$\begin{aligned}\frac{\partial s_x(y)}{\partial y_1}=&F_1(f(y_1),y_1,f(x_1),x_1)f'(y_1)\\&+F_2(f(y_1),y_1,f(x_1),x_1).\end{aligned}\tag{A.9}$$

$$\begin{aligned}\frac{\partial s_y(x)}{\partial y_1}=&F_3(f(x_1),x_1,f(y_1),y_1)f'(y_1)\\&+F_4(f(x_1),x_1,f(y_1),y_1).\end{aligned}\tag{A.10}$$

For the second derivatives, we find

$$\begin{aligned}\frac{\partial^2 s_x(y)}{\partial y_1^2}\Big|_*=&[F_{11}(f(y_1),y_1,f(x_1),x_1)f'(y_1)^2\\&+2F_{12}(f(y_1),y_1,f(x_1),x_1)f'(y_1)\\&+F_1(f(y_1),y_1,f(x_1),x_1)f''(y_1)\\&+F_{22}(f(y_1),y_1,f(x_1),x_1)]|_*\end{aligned}\tag{A.11}$$

and

$$\begin{aligned}\frac{\partial^2 s_y(x)}{\partial y_1^2}\Big|_*=&(F_{33}(f(y_1),y_1,f(y_1),y_1)f'(y_1)^2\\&+2F_{34}(f(y_1),y_1,f(y_1),y_1)f'(y_1)\\&+F_{44}(f(y_1),y_1,f(y_1),y_1)\\&+F_3(f(y_1),y_1,f(y_1),y_1)f''(y_1))|_*.\end{aligned}\tag{A.12}$$

References

Antonovics, J., Thrall, P.H., 1994. Cost of resistance and the maintenance of genetic-polymorphism in host-pathogen systems. Proc. R. Soc. London B 257, 105–110.

Apaloo, J., 1977. Revisiting strategic models of evolution: the concept of neighborhood invader strategies. Theor. Popul. Biol. 52, 71–77.

Boots, M., Begon, M., 1993. Trade-offs with resistance to a granulosis virus in the Indian meal moth, examined by a laboratory evolution experiment. Funct. Ecol. 7, 528–534.

Boots, M., Bowers, R.G., 1999. Three mechanisms of host resistance to microparasites—avoidance, recovery and tolerance—show different evolutionary dynamics. J. Theor. Biol. 201, 13–23.

Boots, M., Bowers, R.G., 2004. The evolution of resistance through costly acquired immunity. Proc. R. Soc. London B 271, 715–723.

Boots, M., Haraguchi, Y., 1999. The evolution of costly resistance in host-parasite systems. Am. Nat. 153, 359–370.

Bowers, R.G., White, A., 2002. The adaptive dynamics of Lotka-Volterra systems with trade-offs. Math. Biosci. 175, 67–81.

Bowers, R.G., Boots, M., Begon, M., 1994. Life-history trade-offs and the evolution of pathogen resistance: competition between host strains. Proc. R. Soc. London B 257, 247–253.

Bowers, R.G., White, A., Boots, M., Geritz, S.A.H., Kisdi, E., 2003. Evolutionary branching/speciation: contrasting results from systems with explicit or emergent carrying capacities. Evol. Ecol. Res. 5, 883–891.

De Mazancourt, C., Dieckmann, U., 2004. Trade-off geometries and frequency-dependent selection. Am. Nat., in press.

Dercole, F., 2002. Evolutionary dynamics through bifurcation analysis: methods and applications. Thesis, Politechnico di Milan.

Dieckmann, U., Law, R., 1996. The dynamical theory of coevolution: a derivation from stochastic ecological processes. J. Math. Biol. 34, 579–612.

Doebeli, M., Dieckmann, U., 2000. Evolutionary branching and sympatric speciation caused by different types of ecological interactions. Am. Nat. 156, S77–S101.

Gatto, M., 1993. The evolutionary optimality of oscillatory and chaotic dynamics in simple population models. Theor. Popul. Biol. 43, 310–336.

Geritz, S.A.H., 2004. Resident-invader dynamics and the coexistence of similar strategies. J. Math. Biol., in press.

Geritz, S.A.H., Metz, J.A.J., Kidsi, E., Meszena, G., 1997. Dynamics of adaptation and evolutionary branching. Phys. Rev. Lett. 78, 2024–2027.

Geritz, S.A.H., Kisdi, E., Meszena, G., Metz, J.A.J., 1998. Evolutionary singular strategies and the adaptive growth and branching of the evolutionary tree. Evol. Ecol. 12, 35–57.

Geritz, S.A.H., Gyllenberg, M., Jacobs, F.J.A., Parvinen, K., 2002. Invasion dynamics and attractor inheritance. J. Math. Biol. 44, 548–560.

Holling, C.S., 1959. The components of predation as revealed by a study of small-mammal predation of the European pine sawfly. Can. Entomol. 91, 293–320.

Kisdi, E., 1999. Evolutionary branching under asymmetric competition. J. Theor. Biol. 197, 149–162.

Kisdi, E., 2001. Long-term adaptive diversity in Levene-type models. Evol. Ecol. Res. 3, 721–727.

Levins, R., 1962. Theory of fitness in heterogeneous environment. 1. The fitness set and the adaptive function. Am. Nat. 96, 361–373.

Marrow, P., Dieckmann, U., Law, R., 1996. Evolutionary dynamics of predator–prey systems: an ecological perspective. J. Math. Biol. 34, 556–578.

Meszéna, G., Kisdi, E., Dieckmann, U., Geritz, S.A.H., Metz, J.A.J., 2000. Evolutionary optimisation models and matrix games in the

unified perspective of adaptive dynamics. IIASA Interim Report IR-00-039.

Metz, J.A.J., Mylius, S.D., Dieckmann, O., 1996. When does evolution optimize? On the relation between types of density dependence and evolutionarily stable life history parameters. IIASA Working Paper WP-96-004.

Metz, J.A.J., Geritz, S.A.H., Meszena, G., Jacobs, F.J.A., Van Heer-Waarden, J.S., 1996. Adaptive dynamics: a geometric study of the consequences of nearly faithful reproduction. In: Van Strien, S.J., Verduyn Lunel, S.M. (Eds.), Stochastic and Spatial Structures of Dynamical Systems. North-Holland, Amsterdam, pp. 183–231.

Rueffler, C., Van Dooren, T.J.M., Metz, J.A.J., 2004. Adaptive walks on changing landscapes: Levin's approach. Theor. Popul. Biol. 65, 165–178.

Stearns, S.C., 1992. The Evolution of Life Histories. Oxford University Press, Oxford.

White, A., Bowers, R.G., 2004. Adaptive dynamics of Lotka–Volterra systems with trade-offs: the role of interspecific parameter dependence in branching. Math. Biosci, in press.